LIMNOLOGY
and
OCEANOGRAPHY: METHODS

ASLO

Limnol. Oceanogr.: Methods 2021

doi: 10.1002/lom3.10425

Making realistic wave climates in low-cost wave mesocosms: A new tool for experimental ecology and biogeomorphology

Eduardo Infantes,[1,2]* **Jaco C. de Smit**,[2,3] **Elena Tamarit**,[1] **Tjeerd J. Bouma**[2,3]

[1]Department of Marine Sciences - Kristineberg, University of Gothenburg, Fiskebäckskil, Sweden
[2]Department of Estuarine and Delta Systems, Royal Netherlands Institute for Sea Research (NIOZ), Yerseke, The Netherlands
[3]Faculty of Geosciences, Utrecht University, Utrecht, The Netherlands

Abstract

Wave flume facilities that are primarily designed for engineering studies are often complex and expensive to operate, and hence not ideal for long-term replicated experiments as commonly used in biology. This study describes a low-cost small wave flume that can be used for biological purposes using fresh- or seawater with or without sediment. The wave flume can be used as a mesocosm to study interactions between wave hydrodynamics and benthic organisms in aquatic ecosystems. The low-costs wave maker (< 2000 USD) allows for experimental setups which can be easily replicated and used for longer term studies; hence the term wave mesocosm. Waves were generated with a pneumatic piston and wave heights ranged between 3 and 6 cm. Maximum orbital flow velocities ranged between 10 and 50 cm s^{-1} representing shallow coastal areas with a short fetch. The system can generate both regular waves (i.e., the wave period and orbital velocity remains constant), using a wave absorber, and irregular waves (i.e., varying wave period and orbital velocity) using a fast push and slow pull motion of the wave paddle. This wave mesocosm system is particularly useful in biogeomorphology to quantify interactions between organisms, sediment, and hydrodynamics and for aquatic ecologist aiming to simulate realistic bed shear stress where short- and long-term experiments (weeks–months) can be replicated.

Hydraulic flumes or open channels have been traditionally used to study fluid dynamics by simulating controlled flow conditions for engineering and physical purposes (Middleton 1965; Dalrymple 1985; Hughes 1993) and to study benthic boundary layers (Nowell and Jumars 1984; Muschenheim et al. 1986; Nowell and Jumars 1987; Boudreau and Jørgensen 2001). Hydraulic flumes are often designed to generate unidirectional flow (currents), oscillatory flow (waves), or a combination of both currents and waves. In environmental studies involving ecological processes, unidirectional flumes have been used for wide range of benthic interactions such as larvae settling (Hendriks et al. 2006), seed transport and trapping (Pereda-Briones et al. 2018; Meysick et al. 2019), microplastic retention (de los Santos et al. 2021), sediment erosion (Dahl et al. 2018), or fish behavior (Jutfelt et al. 2017). Between 1985 and 2019, the number of scientific publications in ecology and environmental science was higher for studies using flumes to generate currents (135 studies), than for flumes generating waves (47 studies, Web of Science, Fig. 1a). Although the use of wave flumes in benthic biology is still less common, there is a growing interest in this field (but see Bouma et al. 2005; Infantes et al. 2011; Ros et al. 2014; and references therein). This publication data suggest that there is rising need for ecological research using wave flumes, to be able to understand the environmental impact of global change on organisms (Koch et al. 2010; La Nafie et al. 2012; Babarro and Carrington 2013; Strain et al. 2015) as well as to progress emergent research areas such as biogeomorphology that describes how the interaction between organisms, sediment, and hydrodynamics build a seascape (Naylor et al. 2002; Stallins 2006).

Most existing wave flume facilities are designed for engineering purposes to study sediment transport, coastal erosion, wave propagation, or test coastal structures during the designing process such as ports, dykes, oil platforms, or boat stability (Hughes 1993). These flumes facilities typically use clean freshwater and are sediment-free. Freshwater flumes hamper studying living marine organisms, which has been resolved by using artificial models to mimic the biological subject (Lowe et al. 2005; Luhar et al. 2010; Luhar et al. 2017). Whereas using mimics allows describing the effects of physical

*Correspondence: eduardo.infantes@marine.gu.se

Additional Supporting Information may be found in the online version of this article.

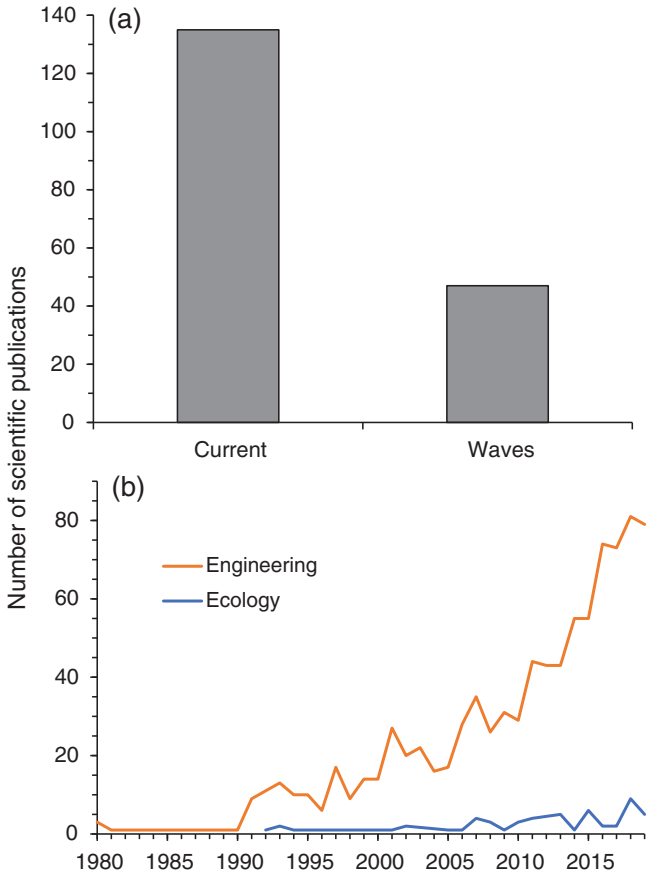

Fig 1. Number of scientific published studies from 1985 to 2019. (**a**) Ecological studies using current and wave flumes. (**b**) Yearly publications in engineering and ecological disciplines using wave flumes (Web of Science).

structures on the fluid dynamics, it does, however, not allow testing the biological response and behavior to hydrodynamic forcing of living organisms (Peralta et al. 2006; Infantes et al. 2011; Strain et al. 2015). In addition, sediment-free facilities limit developing biogeomorphological studies and applications (Naylor et al. 2002; Stallins 2006). To date, the number of published scientific studies using wave flumes is much higher for engineering (1466 studies, 97%) than for ecological studies using live organisms (47 studies, 3% of the total, Fig. 1b), indicating that there is a growing need for wave flume facilities that enable both (1) replicated ecological experiments, in which the response of a living organism can be measured and (2) replicated biogeomorphological experiments, in which the sediment movement can be observed.

Existing wave flumes are commonly large. For example, flumes that generate scaled-down waves or oscillatory currents (i.e., near-bed flow patterns) are in the order of 20 m long, while flumes generating full-sized waves can be up to 300 m long (Thorne et al. 2002; Lara et al. 2016). This results into expensive and complex facilities since large spaces are needed to host the flumes and high maintenance and expertise is required. In addition, large and complex wave generators are used. On the other hand, less expensive and easier to operate smaller U-Tube flumes (Nielsen and Callaghan 2003) or still water tanks with an oscillating tray (Bagnold 1946) can be used to simulate wave orbital excursions, and wave periods at full-scale boundary layer conditions. In these flumes, measurements are performed on specific test scenarios (e.g., interaction between waves and benthic organisms, vegetation types, etc.), but replicated long-term experiments (weeks, months) generally performed in biological and environmental studies cannot be performed (Maza et al. 2015). Since aquatic organisms are affected by hydrodynamics, long-term experiments are needed to understand the growth, development, and adaptation of living organisms when exposed to unidirectional and oscillatory flow regimes. Some studies have been performed to assess organism response to the impact of long-term exposure to unidirectional flow (Wildish and Saulnier 1992; Anthony and Svane 1994; Peralta et al. 2006; de los Santos et al. 2010). For example, Peralta et al. (2006) quantified the impact of three contrasting flow velocities on seagrass development, using 12 mini-flumes. Their results showed that the anchoring system of seagrass was enlarged after 1 month of exposure to high currents. But there are few studies on the long-term effect of wave action. For example, La Nafie et al. (2012) studied the interaction between oscillatory flow and nutrients during 46 d using four wave mesocosms, showing that wave and nutrient interaction was the main driving force affecting survival and morphological properties of seagrass. Using these same wave mesocosms, Strain et al. (2015) showed that high wave exposure and high sediment load reduced plant growth after a 4-month exposure experiment. Performing ecological experiments in wave mesocosms could fill an existing gap in knowledge in this research field.

Designing a hydraulic flume that can be used for all purposes is impossible. In this article, we aim to provide ecologists and biogeomorphologists access to small, low-cost wave flumes that can be used for biological purposes using both fresh- and seawater, either with or without sediment. By being cheap, (< 2000 USD) and being small (3.5 m long) compared to large and complex traditional wave flumes, the experimental setups can be easily replicated allowing for long-term replicated experiments. A pneumatic wave maker was designed as an inexpensive system that could be easily incorporated to mesocosms. The wave flume design was based on La Nafie et al. (2012), and has been further developed to obtain better hydrodynamic conditions, including both regular (i.e., the wave period and orbital velocity remains constant) and irregular waves (i.e., varying wave period and orbital velocity).

Materials and methods

Wave flume design

A seawater flume mesocosm was developed and built at the Royal Netherlands Institute for Sea Research (NIOZ-Yerseke)

and transported to Kristineberg Marine Research Station, Sweden. The flume mesocosm has two parts: a wave generator and a stainless-steel tank of 3.5 m long, 0.6 m wide, and 0.8 m deep. Waves are generated by a pneumatic piston (DNC, Festo®) mounted on a rolling cart, which provided a force of 318 N at a pressure of 4 bar (Fig. 2). The length of each piston stroke is controlled by two pneumatic switches (Roller valve, IMI Norgren®) that limit the movement of the rolling cart. Both switches can be adjusted to increase or reduce the distance of the piston stroke, giving control on the wave's orbital magnitude. The wave frequency is controlled by two high-precision one-way flow control valves (GRP, Festo®) that regulate the forward and backward stroke velocity of the wave paddle. The wave pedal was constructed from 2 cm thick high-pressure compact laminated panel (Trespa®). Door brushes were placed on the sides and bottoms of the wave pedal to minimize the gap between the flume walls and the pedal, and thereby the turbulence created around the sides of the wave pedal.

Wave generation: Regular and irregular waves

Regular and irregular waves were generated by adjusting the water depth, the speed of the wave pedal, and the length of the strokes (Table 1). Two types of regular waves were generated having symmetrical paddle strokes: (1) regular-single waves and (2) regular-continuous waves both in the presence of a wave dampener. In addition, (3) irregular waves were generated by imposing asymmetrical paddle strokes in the absence of a wave dampener. Regular-single waves were generated with a forward paddle stroke followed by a long pause until the wave decayed to prevent a standing wave. Regular-continuous waves were generated by constant forward and backward paddle strokes. Irregular waves were generated by a fast stroke forward, followed by a slow push backward. In the absence of a wave-dampener, the reflections during the slow retraction created chaotic random waves (cf. La Nafie et al. 2012).

Regular-single waves setup was designed to represent solitary waves or the effect of boat wakes in shallow coastal habitats.

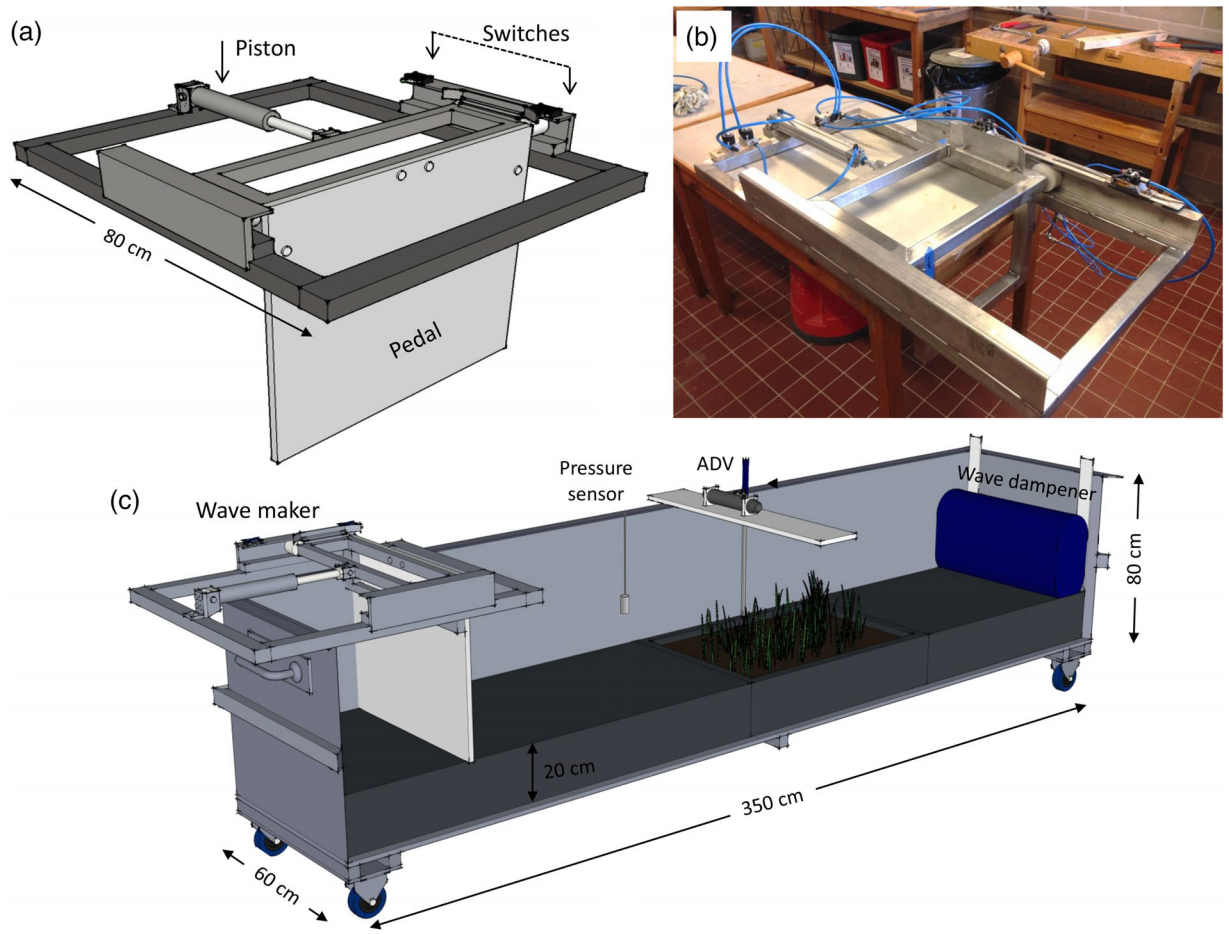

Fig 2. Wave mesocosm. Pneumatic piston wave maker (**a**) diagram, (**b**) photograph, and (**c**) diagram of wave mesocosm with a set of sensors to measure waves (pressure sensor), flow velocity acoustic doppler velocimeter (ADV), and wave dampener. The wave mesocosms shows an example of setup to work with aquatic vegetation where the bottom is raised 20 cm using PVC boxes. All measurements in this study were performed over a flat bottom without the PVC boxes and vegetation.

Table 1. Flume settings for regular and irregular waves. Wave height (H), peak period (T_p), wavelength (L), root mean square orbital velocity (U_{rms}), maximum orbital velocities (U_{max}), thickness of the boundary layer (δ), and turbulent kinetic energy (TKE). Water depth ranged from 21 to 30 cm with a 15° angle wave dampener.

	Regular waves								**Irregular waves**			
	Single waves				**Continuous waves**				**Random**			
Setting number	a	b	c	d	e	f	g	h	i	j	k	l
Depth (cm)	23	23	23	23	23	21	23	30	26	26	26	28
Stroke (cm)	40	40	40	40	31	27	31	35	35	35		
						Waves						
H (cm)	3.5	3.6	3.7	3.5	5.4	4.1	5.7	4.4	2.6	2.4	3.2	3.1
T_p (s)	—	—	—	—	2.2	1.4	1.4	1.4	2.2	1.9	2.0	2.2
L (m)	—	—	—	—	2.7	1.6	1.6	1.8	2.9	2.4	2.6	3.0
Steepness	—	—	—	—	2.0	2.6	3.5	2.5	0.9	1.0	1.2	1.0
						Flow						
U_{rms} (cm s^{-1})	**5**	5	4	4	8	13	20	28	4	**6**	9	16
U_{max} (cm s^{-1})	14	14	14	14	16	23	40	50	10	17	22	33
δ thickness (cm)	—	—	—	—	0.96	0.89	1.16	1.42	0.63	0.72	0.95	1.46
TKE (cm^2 s^{-2})	1.5	1.2	0.9	0.8	10.0	12.5	30.5	16.7	7.0	6.2	12.8	26.8

For example, boat wakes have been shown to cause coastal erosion and making restoration and persistence of marsh vegetation more difficult (Silinski et al. 2016). In addition, Bishop (2008) showed that boat wake exposed sites, had lower amphipod abundance, polychaete abundance, and taxon richness than undisturbed sites. In this wave mesocosm, single waves were generated with a water depth of 23 cm and a paddle stroke of 40 cm. The time between each pedal push was adjusted by setting the pedal pull period from 30, 42, 46, to 66 s. Each pedal push was followed by a series of wave reflections that decayed over time. Due to the presence of a wave dampener, only the first wave heights were fairly constant (3.5–3.7 cm; Table 1).

Regular-continuous waves setup was designed to isolate the effect of one single wave frequency (wavelength) and amplitude (height) on organisms or sediment, instead of intermixing several regular waves of contrasting length and periods. This is a commonly used approach in wave fluid dynamics (Lowe et al. 2005; Luhar et al. 2010; Luhar et al. 2017). Regular waves were generated with paddle strokes of 27–35 cm and water depths of 21–30 cm resulting in four settings which produced wave heights ranging from 4.1 to 5.7 cm, wavelengths from 1.6 to 2.7 cm, and wave periods from 1.4 to 2.2 s (Table 1).

Irregular waves represent a random sea, resulting from the superposition of a number of regular waves with different frequencies and amplitudes. In nature, waves are highly irregular and generating these types of waves in the laboratory implies a closer approximation of natural conditions, albeit with less control on the properties of individual waves compared to the other settings. Irregular waves were generated with a paddle stroke of 35–37 cm, and a fixed fast forward and slower backward paddle motion (cf. La Nafie et al. 2012), producing four settings with wave-heights ranging from 2.4 to 3.1 cm, wavelengths from 2.4 to 3.0 m, and periods from 1.9 to 2.2 s (Table 1).

Regular waves (single and continuous) were damped using six layers of 5 cm thick porous mat placed vertically at the end of the wave flume (Fig. 2c). The vertical layers were designed to reduce reflections of wave energy. The wave dampener had a mild 15° angle slope to increase wave dissipation (Khalilabadi and Bidokhti 2012). Porous mats are a very efficient material absorbing waves (Keulegan 1972) and the performance of vertical wave dampeners could come within a similar range as beach shaped dampeners.

Hydrodynamics characterization

Waves were recorded using a pressure sensor (PTX 1830, Drück) at 25 Hz for 3 min. Wave heights (H, cm) were calculated using the pressure data (Dean and Dalrymple 1984). The typical peak wave period (T_p, s) and frequency (f, Hz), for each wave setting tested, were calculated with a Fourier transformation analysis, which is a common method for analyzing the frequency spectrum of sinusoidal-like wave data. The transformation calculates the strength of each frequency present in the wave data, from which the typical wave period and frequency can be extracted. The wavelength (L, m) was then calculated iteratively for a given depth (D, cm),

$$L = \frac{T_p{}^2 g}{2\pi} \tanh\left(\frac{2\pi D}{L}\right) \quad (1)$$

where g (m s^{-2}) is the gravitational acceleration. Wave steepness indicates the wave linearity and breaking points and was

defined as H_{rms}/L. Instantaneous orbital flow velocities (u, v, w) were measured using an acoustic Doppler velocimeter (Vectrino, Nortek) at 25 Hz for 3 min. Root mean square orbital velocities (U_{rms}, cm s^{-1}) were calculated as,

$$U_{rms} = \sqrt{\frac{1}{N}\sum_{i=1}^{n}\left(u_i^2\right)} \quad (2)$$

where u is the horizontal flow velocity during n measurement points. Vertical profiles of flow velocity were measured for all the wave settings. Each vertical profile consisted of seven measurement points, which were separated by 3 cm at 1, 4, 7, 10, 13, 16, and 19 cm above the bottom. Turbulent kinetic energy per unit mass (TKE, $cm^2\ s^{-2}$) was calculated from the root mean square turbulent velocity components. To be able to calculate the TKE for waves, the turbulence signal has to be separated from the wave signal. A combination of a high-pass and a low-pass Butterworth filter was applied to remove waves and noise from the velocity spectrum, respectively (Smyth and Hay 2003). For the high-pass filter, a cutoff frequency of 1 Hz above the typical wave frequency was used. For the low-pass filter, a cutoff frequency of 6 Hz was chosen. It is worth noting that this method underestimates the TKE, because turbulence at the same frequency as the waves is removed from the signal (Smyth and Hay 2003). The root mean square turbulent velocity was calculated as,

$$\bar{u'} = \left(u'(\bar{t})^2\right)^{1/2} \quad (3)$$

where,

$$u'(t) = u(t) - U(t) \quad (4)$$

where $U(t)$ is the filtered velocity at 1 cm from the bottom. The $\bar{v'}$ and $\bar{w'}$ turbulent velocity components (m s^{-1}) were calculated in the same way. TKE was then calculated as,

$$\mathrm{TKE} = \frac{1}{2}\left(\bar{u'}^2 + \bar{v'}^2 + \bar{w'}^2\right) \quad (5)$$

From this, the bed shear stress (τ, N m^{-2}) can be calculated as (Soulsby 1983),

$$\tau = 0.19\rho\mathrm{TKE} \quad (6)$$

where ρ is the water density (1000 kg m^{-3}). Since the thickness of the boundary layer (δ, cm) over a flat bottom was smaller than 1 cm for all settings, we calculated the theoretical δ following (Schlichting 1979) using a simple approach

$$\delta = 0.37\,\bar{u}^{0.6}\,T_p^{0.8}\,\nu^{0.2} \quad (7)$$

where $\bar{u}$ is the horizontal velocity component, T_p is the peak wave period, and ν is seawater kinematic viscosity. An alternative to Eq. 7 could be to used, δ = 4.61*sqrt ($\nu/\pi/f$) which provides a similar result if $\bar{u}$ is not available (Schlichting and Gersten 2000).

Waves generated in the field—validation measurements

Waves were recorded in the field to compare the range of orbital velocities and corresponding τ to those generated in the wave mesocosm. Wave data were measured in the Bay of Bokevik in the Gullmars Fjord, Sweden (58°14′55.04″N, 11°26′54.30″E) between 4th and 15th of November 2016. The bay is exposed to North–East winds with a fetch of 5-10 km. During the deployment, an event with wind speeds up to 10.3 m s^{-1} was recorded on the 6th of November. An acoustic Doppler velocimeter (ADV, Vector, Nortek) deployed at 2 m depth was used to record wave and flow velocities. The probe was placed looking downward at 15 cm above the bottom, and measurements were taken in 8.5-min bursts every hour, for 4096 records at 8 Hz (Infantes et al. 2012). The wave heights, orbital flow velocities, and wave frequency spectra were calculated for each burst using pressure and acoustic data collected by the instrument. The time-averaged bed shear stress τ can be calculated from the orbital velocity and wave period as follows,

$$\tau = \frac{1}{4}\rho f_w {u_p}^2 \quad (8)$$

where u_p is the significant peak orbital velocity (m s^{-1}) and f_w is the friction factor (–), which is calculated as (Swart 1976),

$$f_w = \exp\left[-5.977 + 5.213*\left\{\frac{\left(\frac{u_p T_p}{2\pi}\right)}{ks}\right\}^{-0.194}\right] \quad (9)$$

where ks is the bed roughness, which for a coastal shallow area with medium sand, and median grain size D_{50} = 250 μm, which is approximately 6.25×10^{-4} m ($2.5D_{50}$).

Assessment

Regular and irregular wave settings in the mesocosm generated maximum orbital flow velocities between 10 and 50 cm s^{-1} and corresponding wave heights from 2.4 to 5.7 cm (Table 1, Supporting Information Fig. S1). For single waves, flow velocities in the profiles ranged within an average of 1.3% vertical variation along the water column (Fig. 3a). This indicates that the hydrodynamic forcing between waves stays constant, making this setting suitable for studying the effects of a specific wave force. For continuous waves, flow velocities in the profiles ranged within an average of 7.4% vertical variation (Fig. 3b), and for irregular waves an average of 10.9% vertical variation (Fig. 3c), indicating that for these settings there is more variation in hydrodynamic forcing which corresponds more to natural wave conditions. The wave pedal generated a

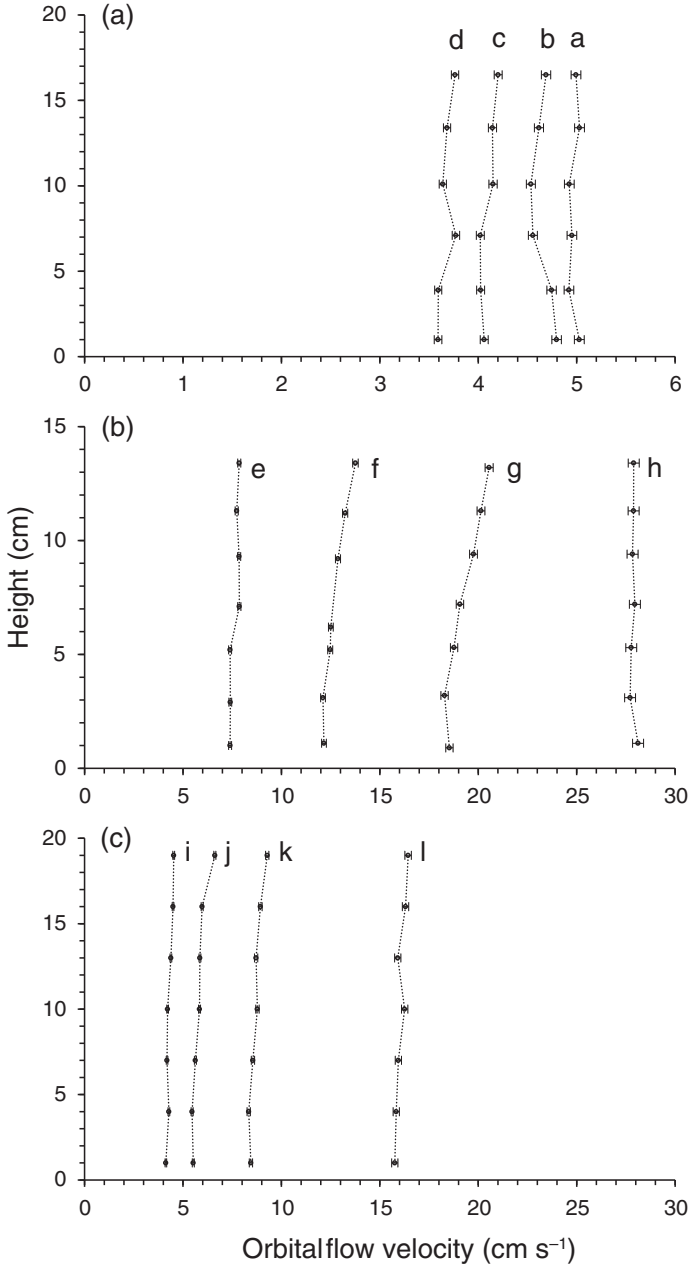

Fig 3. Vertical profiles of flow velocity for each flume setting: (**a**) regular-single waves, (**b**) regular-continuous waves, and (**c**) irregular waves. Error bars indicate the standard deviation.

uniform vertical profile of velocity over the whole water column with a bottom boundary layer smaller than 1 cm for the three types of waves (Fig. 3). The estimated boundary layer thickness over a flat bottom for these wave conditions were also smaller or close to 1 cm (Table 1).

The maximum orbital flow velocities generated by regular continuous waves was higher (16–50 cm s^{-1}) than for irregular waves (10–33 cm s^{-1}, Table 1, Fig. 4). These differences in flow velocities were probably driven by higher wave heights generated for regular waves (4.1–5.7 cm) compared to irregular waves (2.4–3.2 cm) due to wave amplification by reflecting waves (Fig. 5b,c), since peak periods and wavelengths were similar for both settings. Similarly, wave steepness (H/L) was higher for regular continuous waves (2.0–3.5) than for irregular waves (0.9–1.2). Regular single waves generated with a fast pedal stroke followed by a slow push backward reached maximum orbital velocities of 14 cm s^{-1} during the fast stroke, followed by a resting period during which waves gradually declined. The TKE had similar value ranges for both regular continuous waves (10–30.5 cm^2 s^{-2}) and irregular waves (6.2–26.8 cm^2 s^{-2}). TKE values generated at the regular single waves settings were an order of magnitude lower (0.8–1.5 cm^2 s^{-2}), as the energy input (i.e., one paddle stroke per 30–66 s) was also an order of magnitude lower compared to the regular continuous and irregular waves (one paddle stroke per 1.4–2.2 s).

Together with settings of the wave generator, the presence of the wave dampener was another important setting for the wave characteristics of the wave flume. Our design reduced wave energy by allowing percolation of water through the permeable mesh, which thereby reduced wave reflections (Fig. 6). Even though the wave dampener showed a great improvement in reducing wave reflection, there were still some weak reflections present in the most optimal settings. For regular continuous waves, the most dominant wave frequencies show a clear first wave peak, in some cases followed by smaller secondary and tertiary peaks, indicating the presence of reflections (Fig. 5b and Supporting Information Fig. S2). These peaks were however nearly two orders of magnitude lower than the main wave peak. In contrast, for irregular waves, the wave spectrums show typically 3–5 peaks of dominant frequencies of which the energy approximately one order of magnitude lower than the main wave peak, which indicates the initial wave is followed by smaller waves originating by reflection (Fig. 5c). It is however clear that we avoid the formation of a standing wave, by having an asymmetric fast push and slow pull during the generation of irregular waves (Figs. 4, 5c).

Waves recorded in the field during the peak of the wind event (06 November 2016 at 01:00 h) generated waves with a significant wave height of 45 cm and a peak wave frequency of 0.3 Hz, which corresponds to a wave peak period of 3.3 s (Fig. 7). These wave conditions generated orbital velocities of 24 cm s^{-1} near the bottom. As the wave mesocosm can generate orbital velocities up to 50 cm s^{-1}, it can impose both the typical and extreme wave conditions in the shallow parts of fetch-limited bays and estuaries. These properties of the field waves result in a bed shear stress τ of 0.23 N m^{-2}. In comparison, the τ based on the TKE values of the regular continuous and irregular waves with a similar peak orbital velocities (1.25×10^{-3} m^{-2} s^{-2} and 1.28×10^{-3} m^{-2} s^{-2} respectively) is 0.24 N m^{-2}. Thus, the waves generated in the mesocosm have orbital velocity–τ combinations which are similar to those of field waves.

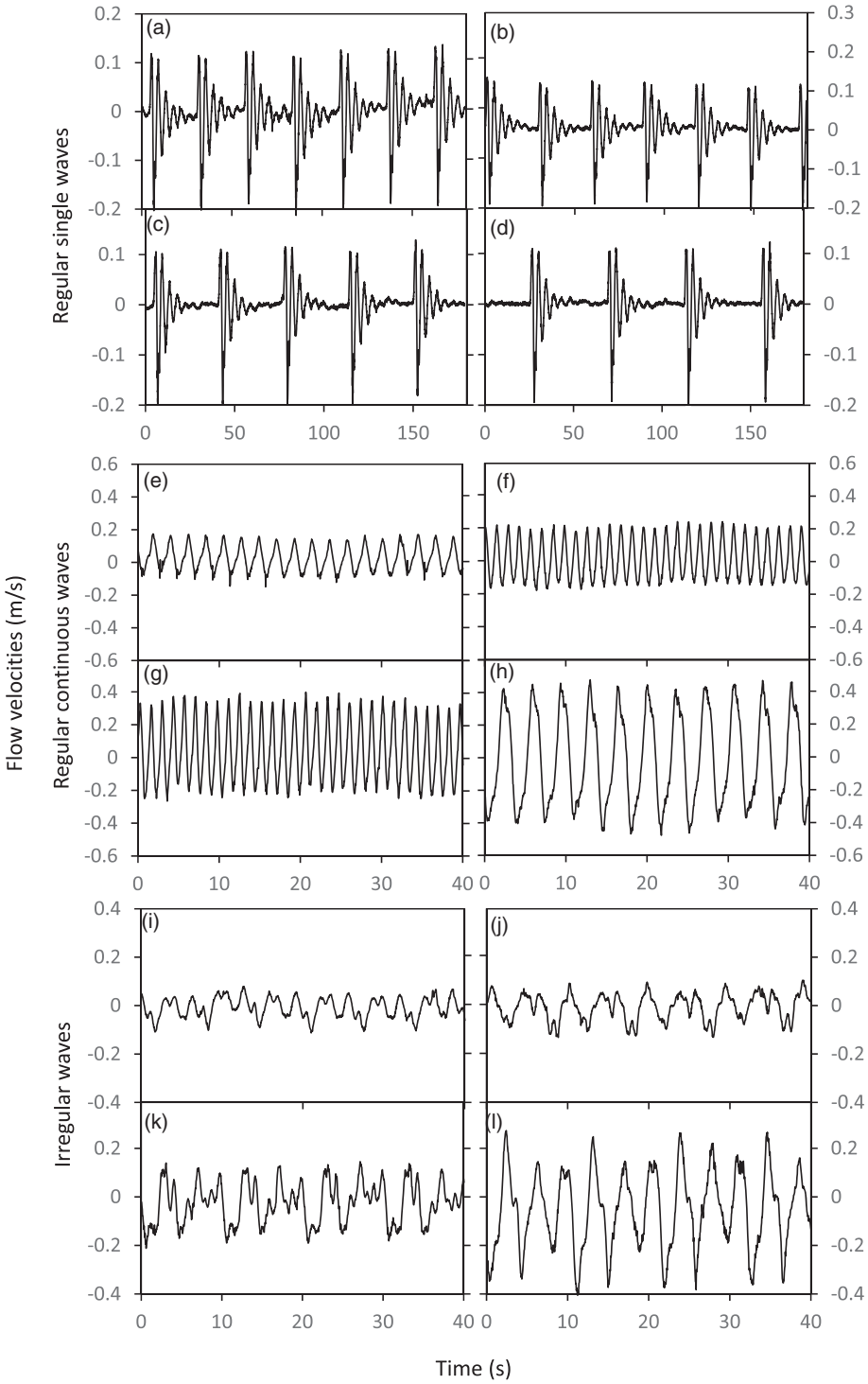

Fig 4. Flow velocities for each flume setting: (**a**–**d**) regular-single waves, (**e**–**h**) regular-continuous waves, and (**i**–**l**) irregular waves. A wave dampener was present with the regular waves settings but was absent for irregular waves. For clarity, 180 s are shown for regular single waves, while for the rest 40 s is shown.

Discussion

This study shows that a range of realistic relevant regular and irregular wave conditions can be generated in a relative small (3.5 m long) and low-cost wave mesocosm (approximately 1700 USD), thereby enabling new experimental possibilities in the fields of aquatic ecology and biogeomorphology. This wave mesocosm is ideal to investigate the effect of long exposures to flow on living organisms, by

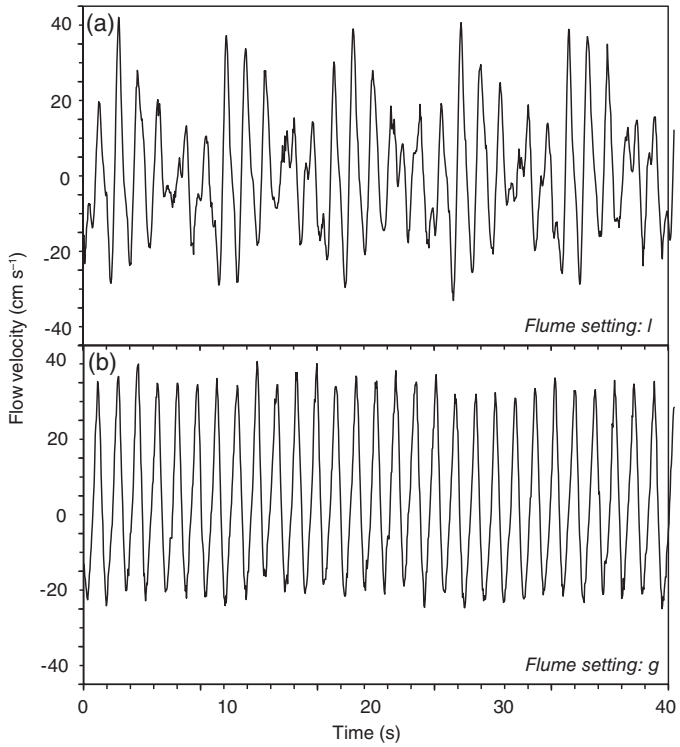

Fig 5. Orbital flow velocities: (**a**) without a wave dampener, resulting in an irregular wave, flume setting l, and (**b**) with a wave dampener, resulting in a regular-continuous wave, flume setting g.

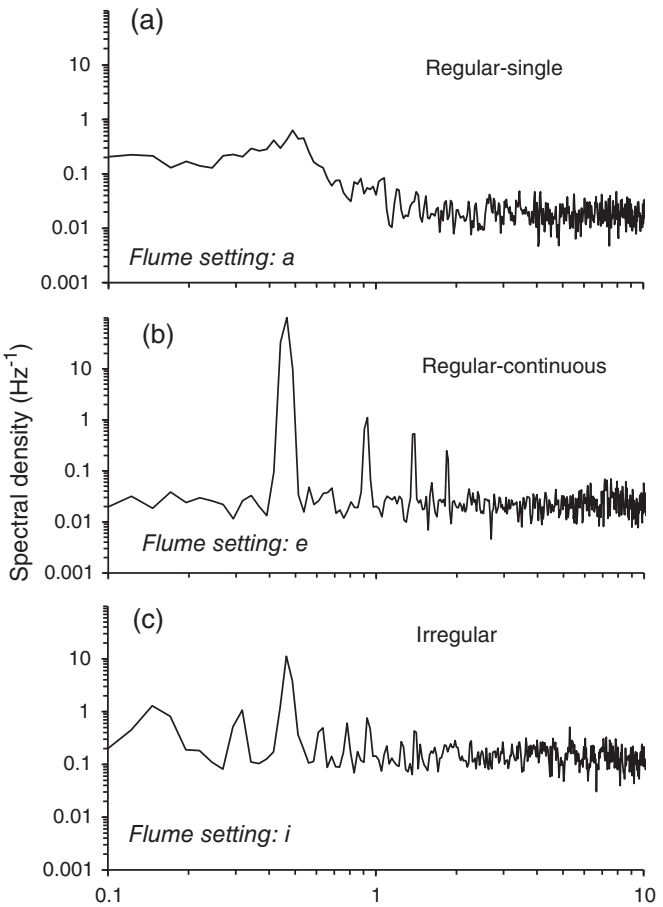

Fig 6. Wave spectrum for different settings: (**a**) regular-single waves, (**b**) regular-continuous wave, and (**c**) irregular waves. A wave dampener was present with the regular waves settings but was absent for irregular waves.

simulating short waves (T_p = 1–3 s) usually present in shallow areas of estuaries, fjords or lakes. Wave parameters were mainly determined by (1) the method of wave generation via the paddle movement and (2) the ability of the wave absorber to reduce reflections. This wave mesocosm system is suitable to study long-term interactions between benthic organisms and wave exposure for a single organism or for a community of organisms. For example, interactions between wave exposure and coastal vegetation (Wolaver et al. 1985; Koch et al. 2010; Infantes et al. 2011; La Nafie et al. 2012), erosion of sediment (Lo et al. 2017; Wang et al. 2017; Marin-Diaz et al. 2020), animal behavior (Stoll et al. 2010), and animal plasticity and adaptations to flow (Trussell 1997; Trussell 2002; Le Pennec et al. 2017). The wave mesocosms has also applications for freshwater ecosystems, for example, in water mixing in lakes and freshwater ecology (Blottière et al. 2017; Hulot et al. 2017). Some specific questions in aquatic ecology and biogeomorphology that could be addressed with the wave mesocosms could include; how waves affect mussel morphology? (Schotanus et al. 2019), how waves affect the survival, morphology, and biomechanics of plants? (Cao et al. 2020), how sediment motion is affected by plant canopies? (Wang et al. 2017; Marin-Diaz et al. 2020), when plant roots reduce erosion? (Lo et al. 2017). Measuring physical parameters in the flume, such as flow velocities, wave, stress and drag forces, sediment dynamics, turbidity, and light attenuation, is possible using a range of sampling techniques (Table 2).

Realistic wave conditions

The wave mesocosm presented here aims to simulate a hydrodynamic stress on the organisms and/or sediment with wave dynamics similar to those in shallow coastal areas. Due to the size however, waves in the mesocosm are scaled down in terms of wave height and wavelength. Scaling is an important issue in physical models and laboratory techniques in coastal engineering studies, where miniature artificial mimics usually represent the real structure to be tested (Hughes 1993). In biological studies however, living organisms (e.g., fish, plants, invertebrates) cannot be scaled down. Therefore, it is usually impossible to recreate a realistic wave height, wavelength, and water depth relative to the organism's size using small flumes. Instead, flow velocities are generally used to simulate wave exposure (Infantes et al. 2011; Ros et al. 2014; Le Pennec et al. 2017). A solution can be to simulate the desired orbital flow velocity (U_b) or maximum orbital velocity (U_{max})

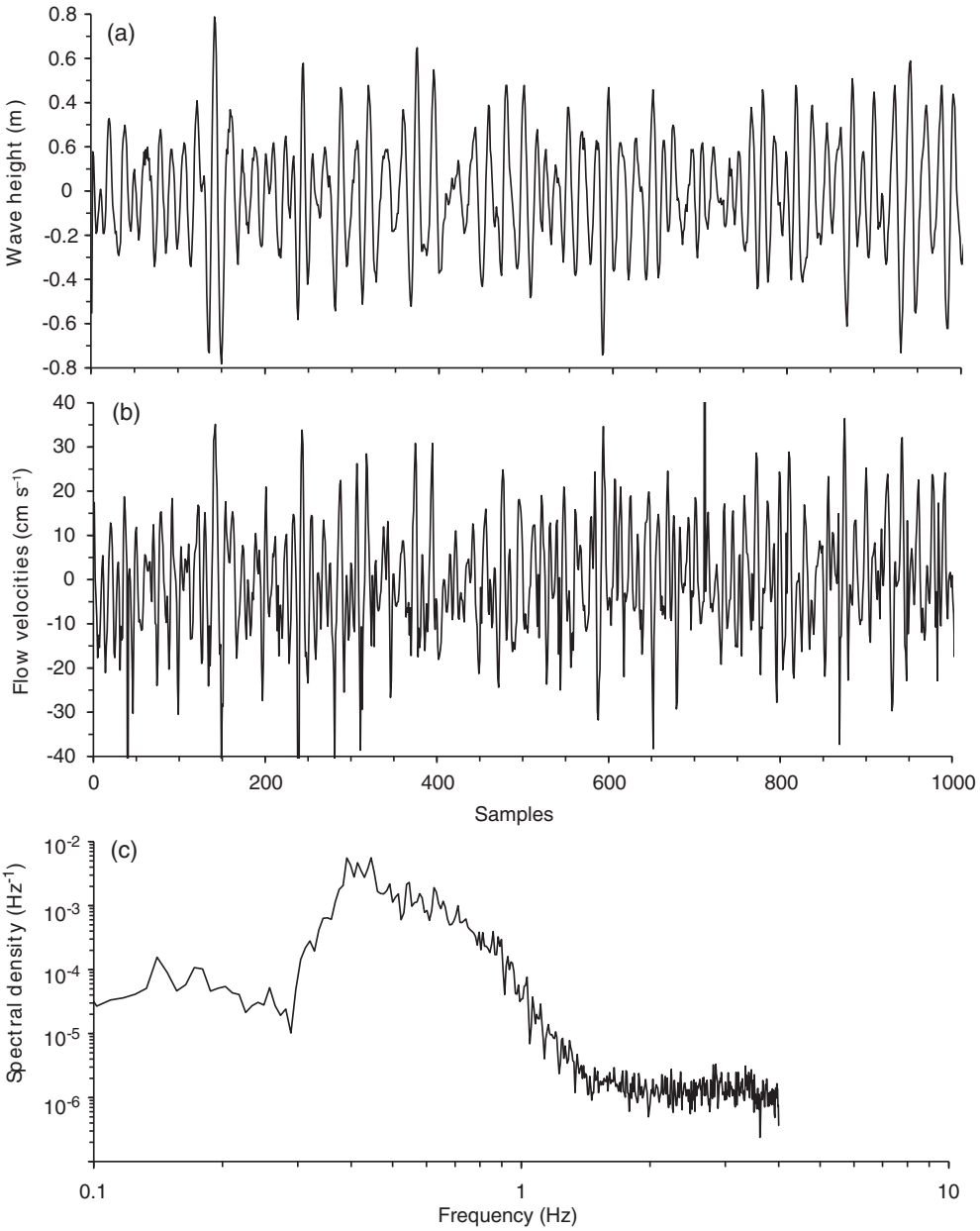

Fig 7. Field wave conditions measured with an acoustic Doppler velocimeter at Bokevik in the Gullmars fjord (1.5 m depth), during a storm event on the 06 November 2016 at 01:00 h. (**a**) Wave heights, (**b**) Orbital velocities, and (**c**) Wave spectrum. For clarity, 1000 samples (125 s) are shown from a burst of 4096 samples at 8 Hz.

that the organisms could be exposed in their natural habitat. The wave mesocosm presented in this study has shown to reproduce mean and maximum orbital flow velocities (0–28 cm s^{-1} and 10–50 cm s^{-1}, respectively). Maximum orbital velocities typically impose the highest drag-force stress on organisms and could determine their survival or fate such as anchoring, breaking strength, or adhesion (Denny 1994; Martone and Denny 2008; Le Pennec et al. 2017). Also, maximum orbital velocities significantly affect sediment erosion because of the nonlinear relation between instantaneous flow velocity and sediment transport. For example, bed load sediment transport depends on instantaneous flow velocity to the power of 3, while suspended sediment transport depends on instantaneous flow velocity to the power of 5 (Kleinhans 2005).

This wave mesocosm was not specifically designed for detailed studies on boundary layer interactions. For these type of studies, larger flumes or U-Tube flumes (Nielsen and Callaghan 2003) are more appropriate to simulate wave orbital excursions at full-scale boundary layer conditions. For studies

Table 2. Methods to measure biogeomorphological parameters in a wave mesocosm.

Parameter	Method	Reference
Flow	Particle image velocimetry	Drucker and Lauder (1999)
	Laser Doppler velocimetry	Koehl (2007); Diplas et al. (2008)
	Acoustic Doppler velocimetry	Infantes et al. (2011); Bouma et al. (2005)
	High speed camera	Videler et al. (1991)
Wave	Pressure sensor	Infantes et al. (2011); Bouma et al. (2005)
	Resistance gauge	Suh et al. (2001); Brevik (1980)
Turbidity	Pump sampling	Baas et al. (2004)
	Fluorometer	Cloutier et al. (2002)
	Light sensor	Aberle et al. (2003)
Force, drag	Torque	Chapman et al. (2014)
	Load cells	Infantes et al. (2011); Bouma et al. (2005)
Sediment	Infrared profiler	Clifford et al. (1995)
	Stereo photography	Hilsenstein (2005); Stojic et al. (1998)
	Optical backscatterance sensors	Ribberink et al. (2001); Widdows et al. (1998)
	Acoustic backscatterance sensors	Thorne et al. (2002); Ribberink et al. (2001)
Nutrients	Pump sampling	Bilger et al. (1995); Beaulieu (2003)

requiring that the boundary layer thickness scales with the size of the organisms (eg. bending stress, food encounter with suspension feeders), this system does not reproduce realistic drag forces in large nonbreaking waves or in breaking waves, due the thin boundary layer developed in the tanks. Instead, this wave mesocosm simulates realistic bed shear stress τ over longer time periods (weeks to months) to answer ecological questions using replicated experiments. Nowell and Jumars (1987) recommended that for reproducing biologically relevant boundary layers in unidirectional flumes, the flume width to depth ratio should be between 5:1 and 10:1. This ratio suggested for unidirectional flumes might not be valid for the wave mesocosm used in this study (ratio 2 : 1), since the water depth is more important for wave propagation. In fact, nearly all flumes violate this rule except for flumes which are specifically used to study large-scale morphological development of rivers (Tal and Paola 2007) and estuaries (Kleinhans et al. 2017), where both sediment and biology need to be scaled down. In a comparison of 12 biological flumes, Jonsson et al. (2006) concluded that the width of the flume should be larger than the width of the study object and the thickness of the boundary layer multiplied by two, so that the wall boundary layers do not influence flow around the object. Each experiment should always require careful consideration about the best suitable flume design and experimental setup. Some experimental studies simply require a large flume where accurate boundary layers and wave conditions are needed to design, parameterize, or test physical models (Hughes 1993). Other studies could be performed on a smaller scale such as low-cost wave mesocosms, where living organisms are exposed to wave action to quantify growth patterns, adaptations to oscillatory flow, behavioral changes, and so on (Stoll et al. 2010; La Nafie et al. 2012; Schotanus et al. 2019). Such studies do not require hydrodynamically accurate wave conditions, but a constant wave induced bottom shear stress over a period of time.

A wave dampener was present with the regular wave settings but was absent for irregular waves. Passive wave absorption systems can be made of materials such as sand, gravel, stones, wire screens, or transversal bars (Khalilabadi and Bidokhti 2012). This wave mesocosm uses a porous screen that can be easily removed and cleaned compared to harder materials such as sand, gravel, and stones. According to Hughes (1993), an optimal wave absorber should have a length between $0.35L$ and $1L$, where L is the maximum wavelength generated. This means the wavelengths generated in this wave mesocosm would require a wave absorber of 1–3 m. It is obviously not useful and possible to include a 3-m dampener in a 3.5-m tank as the working area would become too short. Hence, we used a much smaller vertical wave dampener with high porosity. Fortunately, this gave a much cleaner wave pattern than without a dampener. Some wave reflections were still present in the wave mesocosm despite the wave dampener. Their energy was, however, nearly two orders of magnitude lower than the wave energy compared to one order of magnitude without a dampener (Fig. 5). Given that >> 90% of the hydrodynamic energy comes from the user-imposed wave, which is representative of natural waves in terms of wave period and orbital velocity–bed shear stress (τ) combinations, the hydrodynamics of this wave mesocosm are of sufficiently quality for ecological and biogeomorphological experiments. It should be considered that the porous texture of the damping material could be a substrate for microorganism growth or a trap for fine sediment. Therefore, it should be rinsed and cleaned regularly.

Low-cost wave-mesocosm

The wave maker used in this mesocosm was designed for intermediate and shallow water waves by using a piston that moves a paddle back and forward, generating water motion which is constant over depth (Fig. 3). Piston wave makers have been shown to produce reliable conditions in hydraulic flumes for solitary waves, regular and irregular waves. The total cost of the wave generator presented here was approximately 1700 USD. Individual components: piston (200 USD),

rolling switches × 2 (150 USD), precision valves × 2 (200 USD), pilot valve (50 USD), and tubing and connectors (100 USD). The frame and paddle to hold the wave maker components were built from stainless steel for a cost of approximately 1000 USD. The price of the tank will obviously vary depending on the size and the material used, and the variability in market prices. A minimum tank size of 3 m long and 0.5 m width built from either stainless steel or fiberglass is recommended. This size will allow to have sufficient space (∼ 1 m) between the wave generator, the test section, and the wave dampener. Given the information in this article, building a similar wave mesocosm with a wave generator with a local contractor should be relatively straightforward. However, for those who are uncertain about building their own system, custom-made systems can be designed and constructed by NIOZ (contact tjeerd.bouma@nioz.nl).

A constant supply of compressed air is needed to run the wave generator. Variations in the main air pressure supply can modify the velocity of the wave generator, as this directly influences the paddle force. The system can run with compressed air from compressors (lubricated and filtered) and gas cylinders such as scuba diving tanks fitted with a manifold to reduce the air pressure to 10 bars. In outdoor cold climates with temperatures below 2°C, the piston may however freeze due to adiabatic cooling. In this case, an electric cylinder could be used instead of a pneumatic cylinder. Another advantage of an electric cylinder is that the precision of the stroke and wave frequency is higher, but with the disadvantage of a more costly (∼ 3× the cost of a pneumatic system) and complex system which may also be more sensitive to corrosion when using salt water given the presence of electronic components.

In conclusion, our wave mesocosm offers a low-cost setup that can create sufficiently realistic hydrodynamics such as a range of regular and irregular waves to explore benthic biological and biogeomorphological processes. Due to the small size and low cost compared to larger flume facilities designed for engineering purposes, it is ideal to perform long-term replicated biological and biogeomorphological studies aimed to simulate short wave conditions (T_p = 1–3 s) and maximum orbital velocities (10–50 cm s^{-1}) usually present in shallow areas of estuaries, fjords, or lakes.

References

Aberle, J., V. Nikora, S. McLean, C. Doscher, I. McEwan, M. Green, D. Goring, and J. Wash. 2003. Straight benthic flow-through flume for in situ measurement of cohesive sediment dynamics. Journal of Hydraulic Engineering-Asce **129**: 63–67. doi:10.1061/(ASCE)0733-9429

Anthony, K. R. N., and I. Svane. 1994. Effects of flow-habitat on body size and reproductive patterns in the sea anemone *Metridium senile* in the Gullmarsfjord, Sweden. Mar. Ecol. Prog. Ser. **113**: 257–269. doi:10.3354/meps113257

Babarro, J. M. F., and E. Carrington. 2013. Attachment strength of the mussel *Mytilus galloprovincialis*: Effect of habitat and body size. J. Exp. Mar. Biol. Ecol. **443**: 188–196. doi:10.1016/j.jembe.2013.02.035

Baas, J. H., W. Van Kesteren, and G. Postma. 2004. Deposits of depletive high-density turbidity currents: a flume analogue of bed geometry, structure and texture. Sedimentology **51**: 1053–1088. doi:10.1111/j.1365-3091.2004.00660.x

Bagnold, R. A. 1946. Motion of waves in shallow water. Interaction between waves and sand bottoms. *Proceedings of the Royal Society of London. Series A. Mathematical and Physical Sciences*. **187** (1008): 1–18. doi:10.1098/rspa.1946.0062.

Beaulieu, S. E. 2003. Resuspension of phytodetritus from the sea floor: A laboratory flume study. Limnology and Oceanography **48**: 1235–1244. doi:10.4319/lo.2003.48.3.1235

Bilger, R. W., and M. J. Atkinson. 1995. Effects of nutrient loading on mass-transfer rates to a coral-reef community. Limnology and Oceanography **40**: 279–289. doi:10.4319/lo.1995.40.2.0279

Bishop, M. J. 2008. Displacement of epifauna from seagrass blades by boat wake. J. Exp. Mar. Biol. Ecol. **354**: 111–118. doi:10.1016/j.jembe.2007.10.013

Blottière, L., M. Jaffar-Bandjee, S. Jacquet, A. Millot, and F. D. Hulot. 2017. Effect of water column mixing on freshwater ecosystems: A mesocosm experiment. Freshw. Biol. **62**: 161–177. doi:10.1111/fwb.12859

Boudreau, B., and B. Jørgensen. 2001. The benthic boundary layer: Transport processes and biogeochemistry. New York, NY: Oxford University Press.

Bouma, T. J., M. B. De Vries, E. Low, G. Peralta, I. C. Tánczos, J. van de Koppel, and P. M. J. Herman. 2005. Trade-offs related to ecosystem engineering: A case study on stiffness of emerging macrophytes. Ecology **86**: 2187–2199. doi:10.1890/04-1588

Brevik, I., and B. Aas. (1980) Flume experiment on waves and currents .1. Rippled Bed. Coastal Engineering **3**: 149-177. doi:10.1016/0378-3839(79)90019-X

Cao, H., Z. Zhu, R. James, P. M. J. Herman, L. Zhang, L. Yuan, and T. J. Bouma. 2020. Wave effects on seedling establishment of three pioneer marsh species: Survival, morphology and biomechanics. Ann. Bot. **125**: 345–352. doi:10.1093/aob/mcz136

Chapman, J. A., J. S. Gulliver, and B. N. Wilson. 2014. Flume instrumentation for measurement of drag on flexible elements under waves. Experiments in Fluids **55**: 1715. doi:10.1007/s00348-014-1715-7

Clifford, N. J., K. S. Richards, R. A. Brown, and S. N. Lane. 1995. Laboratory and field assessment of an infrared turbidity probe and its response to particle size and variation in suspended sediment concentration. Hydrological Sciences Journal **40**: 771–791. doi:10.1080/02626669509491464

Cloutier, D., C. L. Amos, P. R. Hill, and K. Lee. 2002. Oil erosion in an annular flume by seawater of varying turbidities: A critical bed shear stress approach. Spill Science &

Technology Bulletin **8**: 83–93. doi:10.1016/S1353-2561(02)00115-9

Dahl, M., E. Infantes, R. Clevesjö, H. W. Linderholm, M. Björk, and M. Gullström. 2018. Increased current flow enhances the risk of organic carbon loss from *Zostera marina* sediments: Insights from a flume experiment. Limnol. Oceanogr. **63**: 2793–2805. doi:10.1002/lno.11009

Dalrymple, R. A. 1985. Introduction to physical modelling in coastal engineering. doi:10.1201/9780203743379

de los Santos, C. B., F. G. Brun, T. J. Bouma, J. J. Vergara, and J. L. Perez-Llorens. 2010. Acclimation of seagrass *Zostera noltii* to co-occurring hydrodynamic and light stresses. Mar. Ecol. Prog. Ser. **398**: 127–135. doi:10.3354/meps08343

de los Santos, C. B., A. S. Krång, and E. Infantes. 2021. Microplastic retention by marine vegetated canopies: Simulations with seagrass meadows in a hydraulic flume. Environmental Pollution. **269**: 116050. doi:10.1016/j.envpol.2020.116050.

Dean, R., and R. Dalrymple. World Scientific; 1984. Water wave mechanics for engineers and scientists. Series on ocean engineering, v. **2**. doi:10.1142/1232.

Denny, M. 1994. Extreme drag forces and the survival of wind- and water-swept organisms. J. Exp. Biol. **194**: 97–115. https://jeb.biologists.org/content/194/1/97.

Diplas, P., C. L. Dancey, A. O. Celik, M. Valyrakis, K. Greer, and T. Akar. 2008. The role of impulse on the initiation of particle movement under turbulent flow conditions. Science **322**: 717–720. doi:10.1126/science.1158954

Drucker, E. G., and G. V. Lauder. 1999. Locomotor forces on a swimming fish: Three-dimensional vortex wake dynamics quantified using digital particle image velocimetry. Journal of Experimental Biology **202**: 2393–2412.

Hendriks, I., L. Vanduren, and P. Herman. 2006. Turbulence levels in a flume compared to the field: Implications for larval settlement studies. J. Sea Res. **55**: 15–29. doi:10.1016/j.seares.2005.09.005

Hilsenstein, V. 2005. Surface reconstruction of water waves using thermographic stereo imaging. Image and Vision Computing New Zealand, CiteSeer 2, p. 1–6.

Hughes, S. A. 1993. Physical models and laboratory techniques in coastal engineering. Advanced series on ocean engineering, v. **7**. World Scientific Publishing. https://www.worldscientific.com/worldscibooks/10.1142/2154.

Hulot, F. D., M. Rossi, B. Verdier, J.-. P. Urban, L. Blottière, F. Madricardo, and B. Decencière. 2017. Mesocosms with wavemakers: A new device to study the effects of water mixing on lake ecology. Limnol. Oceanogr.: Methods **15**: 154–165. doi:10.1002/lom3.10149

Infantes, E., A. Orfila, G. Simarro, J. Terrados, M. Luhar, and H. Nepf. 2012. Effect of a seagrass (*Posidonia oceanica*) meadow on wave propagation. Mar. Ecol. Prog. Ser. **456**: 72–72. doi:10.3354/meps09754.

Infantes, E., A. Orfila, T. J. Bouma, G. Simarro, and J. Terrados. 2011. *Posidonia oceanica* and *Cymodocea nodosa* seedling tolerance to wave exposure. Limnol. Oceanogr **56**: 2223–2232. doi:10.4319/lo.2011.56.6.2223

Jonsson, P. R., et al. 2006. Making water flow: A comparison of the hydrodynamic characteristics of 12 different benthic biological flumes. Aquat. Ecol. **40**: 409–438. doi:10.1007/s10452-006-9049-z

Jutfelt, F., J. Sundin, G. D. Raby, A. S. Krang, and T. D. Clark. 2017. Two-current choice flumes for testing avoidance and preference in aquatic animals. Methods Ecol. Evol. **8**: 379–390.

Keulegan, G. 1972. Wave damping effects of fibrous screens. U.S. Army Engineer Waterways Experiment Station H-72-2.

Khalilabadi, M. R., and A. A. Bidokhti. 2012. Design and construction of an optimum wave flume. J. Appl. Fluid Mech. **5**: 99–103.

Kleinhans, M. G. 2005. Flow discharge and sediment transport models for estimating a minimum timescale of hydrological activity and channel and delta formation on Mars. J. Geophys. Res. Planets **110**: (E12003). doi:10.1029/2005JE002521

Kleinhans, M. G., J. R. F. W. Leuven, L. Braat, and A. Baar. 2017. Scour holes and ripples occur below the hydraulic smooth to rough transition of movable beds. Sedimentology **64**: 1381–1401. doi:10.1111/sed.12358

Koch, E. W., M. S. Ailstock, D. M. Booth, D. J. Shafer, and A. D. Magoun. 2010. The role of currents and waves in the dispersal of submersed angiosperm seeds and seedlings. Restor. Ecol. **18**: 584–595. doi:10.1111/j.1526-100X.2010.00698.x.

Koehl, M. R. A. 2007. Mini review: Hydrodynamics of larval settlement into fouling communities. Biofouling **23**: 357–368. doi:10.1080/08927010701492250

La Nafie, Y. A., C. B. de los Santos, F. G. Brun, M. M. van Katwijk, and T. J. Bouma. 2012. Waves and high nutrient loads jointly decrease survival and separately affect morphological and biomechanical properties in the seagrass *Zostera noltii*. Limnol. Oceanogr. **57**: 1664–1672. doi:10.4319/lo.2012.57.6.1664

Lara, J. L., M. Maza, B. Ondiviela, J. Trinogga, I. J. Losada, T. J. Bouma, and N. Gordejuela. 2016. Large-scale 3-D experiments of wave and current interaction with real vegetation. Part 1: Guidelines for physical modeling. Coast. Eng. **107**: 70–83. doi:10.1016/j.coastaleng.2015.09.012

Le Pennec, G., R. K. Butlin, P. R. Jonsson, A. I. Larsson, J. Lindborg, E. Bergström, A. M. Westram, and K. Johannesson. 2017. Adaptation to dislodgement risk on wave-swept rocky shores in the snail *Littorina saxatilis*. PLoS One **12**(10): e0186901. doi:10.1371/journal.pone.0186901

Lo, V. B., T. J. Bouma, J. van Belzen, C. Van Colen, and L. Airoldi. 2017. Interactive effects of vegetation and sediment properties on erosion of salt marshes in the Northern Adriatic Sea. Mar. Environ. Res. **131**: 32–42. doi:10.1016/j.marenvres.2017.09.006

Lowe, R. J., J. R. Koseff, and S. G. Monismith. 2005. Oscillatory flow through submerged canopies: 1. Velocity structure. J. Geophys. Res. **110**: 1–17. doi:10.1029/2004JC002788.

Luhar, M., S. Coutu, E. Infantes, S. Fox, and H. Nepf. 2010. Wave-induced velocities inside a model seagrass bed. J. Geophys. Res. **115**: 1–15. doi:10.1029/2010JC006345.

Luhar, M., E. Infantes, and H. Nepf. 2017. Seagrass blade motion under waves and its impact on wave decay. J. Geophys. Res. Oceans **122**: 3736–3752. doi:10.1002/2017JC012731

Marin-Diaz, B., T. J. Bouma, and E. Infantes. 2020. Role of eelgrass on bed-load transport and sediment resuspension under oscillatory flow. Limnol. Oceanogr. **65**: 426–436. doi:10.1002/lno.11312

Martone, P. T., and M. W. Denny. 2008. To break a coralline: Mechanical constraints on the size and survival of a wave-swept seaweed. J. Exp. Biol. **211**: 3433–3441. doi:10.1242/jeb.020495

Maza, M., J. L. Lara, I. J. Losada, B. Ondiviela, J. Trinogga, and T. J. Bouma. 2015. Large-scale 3-D experiments of wave and current interaction with real vegetation. Part 2: Experimental analysis. Coast. Eng. **106**: 73–86. doi:10.1016/j.coastaleng.2015.09.010

Meysick, L., E. Infantes, and C. Bostrom. 2019. The influence of hydrodynamics and ecosystem engineers on eelgrass seed trapping. PLoS One **14**: e0222020. doi:10.1371/journal.pone.0222020

Middleton, G. V. 1965. Antidune cross-bedding in a large flume. J. Sediment. Petrol. **35**(4): 922–927. doi:10.1306/74D713AC-2B21-11D7-8648000102C1865D.

Muschenheim, D. K., J. Grant, and E. L. Mills. 1986. Flumes for benthic ecologists - theory, construction and practice. Mar. Ecol. Prog. Ser. **28**: 185–196. doi:10.3354/meps028185

Naylor, L. A., H. A. Viles, and N. E. A. Carter. 2002. Biogeomorphology revisited: Looking towards the future. Geomorphology **47**: 3–14. doi:10.1016/S0169-555X(02)00137-X

Nielsen, P., and D. P. Callaghan. 2003. Shear stress and sediment transport calculations for sheet flow under waves. Coast. Eng. **47**: 347–354. doi:10.1016/S0378-3839(02)00141-2

Nowell, A. R. M., and P. A. Jumars. 1984. Flow environmenst of aquatic benthos. Annu. Rev. Ecol. Syst. **15**: 303–328. doi:10.1146/annurev.es.15.110184.001511

Nowell, A. R. M., and P. A. Jumars. 1987. Flumes: Theoretical and experimental considerations for simultion of benthic environments. Oceanogr. Mar. Biol. Annu. Rev. **25**: 91–112.

Peralta, G., F. G. Brun, J. L. Pérez-lloréns, and T. J. Bouma. 2006. Direct effects of current velocity on the growth, morphometry and architecture of seagrasses: A case study on *Zostera noltii*. Mar. Ecol. Prog. Ser. **327**: 135–142. doi:10.3354/meps327135

Pereda-Briones, L., E. Infantes, A. Orfila, F. Tomas, and J. Terrados. 2018. Dispersal of seagrass propagules: Interaction between hydrodynamics and substratum type. Mar. Ecol. Prog. Ser. **593**: 47–59. doi:10.3354/meps12518

Ribberink, J., Dohmen-Janssen, C., Mclean, S., Vincent, C. (2001) Near-bed sand transport mechanisms under waves: a large scale flume experiment (SISTEX) Proceedings of the 27th International Conference on Coastal Engineering 2000, Volume IV, 3263-3276, Sydney, Australia.

Ros, À., J. Colomer, T. Serra, D. Pujol, M. Soler, and X. Casamitjana. 2014. Experimental observations on sediment resuspension within submerged model canopies under oscillatory flow. Cont. Shelf Res. **91**: 220–231. doi:10.1016/j.csr.2014.10.004

Schlichting, H. 1979. Boundary layer theory, 7th Edition. McGraw-Hill.

Schlichting, H., and K. Gersten. 2000. Boundary-layer theory. Springer. doi:10.1007/978-3-662-52919-5.

Schotanus, J., J. J. Capelle, L. Leuchter, J. van de Koppel, and T. J. Bouma. 2019. Mussel seed is highly plastic to settling conditions: The influence of waves versus tidal emergence. Mar. Ecol. Prog. Ser. **624**: 77–87. doi:10.3354/meps13039

Silinski, A., et al. 2016. Effects of contrasting wave conditions on scour and drag on pioneer tidal marsh plants. Geomorphology **255**: 49–62. doi:10.1016/j.geomorph.2015.11.021

Smyth, C., and A. E. Hay. 2003. Near-bed turbulence and bottom friction during SandyDuck97. J. Geophys. Res. Atmos. **108**(C6):3197. doi:10.1029/2001JC000952

Soulsby, R. 1983. Chapter 5: The bottom boundary layer of shelf seas, p. 189–266.*In* Elsevier oceanography series, v. **35**. doi:10.1016/S0422-9894(08)70503-8.

Stallins, J. A. 2006. Geomorphology and ecology: Unifying themes for complex systems in biogeomorphology. Geomorphology **77**: 207–216. doi:10.1016/j.geomorph.2006.01.005

Stoll, S., W. N. Probst, R. Eckmann, and P. Fischer. 2010. A mesocosm experiment investigating the effects of substratum quality and wave exposure on the survival of fish eggs. Aquat. Sci. **72**: 509–517. doi:10.1007/s00027-010-0152-9

Strain, E. M., J. van Belzen, J. van Dalen, T. J. Bouma, and L. Airoldi. 2015. Management of local stressors can improve the resilience of marine canopy algae to global stressors. PLoS One **10**: e0120837. doi:10.1371/journal.pone.0120837

Stojic, M., J. Chandler, P. Ashmore, and J. Luce. 1998. The assessment of sediment transport rates by automated digital photogrammetry. Photogrammetric Engineering and Remote Sensing **64**: 387–395.

Suh, K. D., W. S. Park, and B. S. Park. 2001. Separation of incident and reflected waves in wave-current flumes. Coastal Engineering **43**: 149–159. doi:10.1016/S0378-3839(01)00011-4

Swart, D. 1976. Computation of long shore transport. Report No. R968. Delft Hydraulics Laboratory.

Tal, M., and C. Paola. 2007. Dynamic single-thread channels maintained by the interaction of flow and vegetation. Geology **35**: 347–350. doi:10.1130/G23260A.1

Thorne, P. D., J. J. Williams, and A. G. Davies. 2002. Suspended sediments under waves measured in a large-scale flume facility. J. Geophys. Res. Oceans **107**: 4-1–4-16.

Thorne, P. D., J. J. Williams, and A. G. Davies. 2002. Suspended sediments under waves measured in a large-scale flume facility. Journal of Geophysical Research-Oceans **107**: C8. doi:10.1029/2001JC000988

Trussell, G. C. 1997. Phenotypic plasticity in the foot size of an intertidal snail. Ecology **78**: 1033–1048.

Trussell, G. C. 2002. Evidence of countergradient variation in the growth of an intertidal snail in response to water velocity. Mar. Ecol. Prog. Ser. **243**: 123–131. doi:10.3354/meps243123

Videler, J. J., and C. S. Wardle. 1991. Fish swimming stride by stride - Speed limits and endurance. Reviews in Fish Biology and Fisheries **1**: 23–40. doi:10.1007/BF00042660

Wang, H., and others. 2017. Zooming in and out: Scale dependence of extrinsic and intrinsic factors affecting salt marsh erosion. J. Geophys. Res. Earth Surf. **122**: 1455–1470. doi:10.1002/2016JF004193

Wildish, D. J., and A. M. Saulnier. 1992. The effect of velocity and flow direction on the growth of juvenile and adult giant scallops. J. Exp. Mar. Biol. Ecol. **155**: 133–143. doi:10.1016/0022-0981(92)90032-6

Wolaver, T., and others. 1985. The flume design - a methodology for evaluating material fluxes between a vegetated salt-marsh and the adjacent tidal creek. J. Exp. Mar. Biol. Ecol. **91**: 281–291. doi:10.1016/0022-0981(85)90182-0

Widdows, J., M. D. Brinsley, P. N. Salkeld, and M. Elliott. 1998. Use of annular flumes to determine the influence of current velocity and bivalves on material flux at the sediment-water interface. Estuaries **21**: 552–559. doi:10.2307/1353294

Acknowledgments

E. Infantes will like to thank FORMAS grant Dnr. 231-2014-735 and funds provided by the Royal Society of Arts and Sciences in Gothenburg. Thanks to the staff of Kristineberg Research Station for providing their great facilities. The idea to develop the wave-flume/wave-mesocosm was initiated by T. J. Bouma at NIOZ. We gratefully acknowledge Bert Sinke for making the original flume design and the NMF-team at NIOZ who constructed the flume and Selwyn Hoeks for the flume diagrams. For question on having a wave-mesocosm to be built at NIOZ, contact tjeerd.bouma@nioz.nl.

Conflict of Interest

None declared.

Submitted 12 May 2020
Revised 08 February 2021
Accepted 18 February 2021

Associate editor: George Waldbusser